

Enhanced Distillate Yield in Pyramid Solar Still Due to the Coupling Effect of Flat Plate Collector and Shallow Solar Pond

S. Mari Vignesh^a, M. Anbu Saravanan^a, V. Shanmugapriya^a, R. Jayaprakash^b and B. Selvakumar^{a*}

^a Dept. of Physics, Kalasalingam Academy of Research and Education, Krishnankoil, India

^b Dept. of Physics, Sri Ramakrishna Mission Vidhyalaya College of Arts and Science, Coimbatore, Tamil Nadu, India

Abstract

Impact of flat plate collector and shallow solar pond in enhancing the productive yield of pyramid solar still has been carried out. Heat transfer modes, efficiency and performance ratio along with thermophysical properties such as thermal conductivity, dynamic viscosity and density were also predicted for pyramid solar still under three modes of study. Distillate yield observed for pyramid solar still individually, pyramid still coupled with FPC and pyramid still coupled with SSP is about 2.366 litre/m², 3.169 litre/m² and 3.731 litre/m². Instantaneous efficiency observed during the study is in the range of 7.52% to 32.73%, 2.41% to 9.01% and 2.42% to 11.28% for the pyramid still performance study alone, combined with FPC and combined with SSP. Even though the instantaneous efficiency in this mode is reduced than the pyramid solar still, the distillate water collection rate is increased. Thermal conductivity of water is analyzed and it is observed in the range of 26.89x10⁻³ Wm⁻² °C⁻¹ to 28.19x10⁻³ Wm⁻² °C⁻¹, 26.95x10⁻³ Wm⁻² °C⁻¹ to 28.46x10⁻³ Wm⁻² °C⁻¹ and 26.97x10⁻³ Wm⁻² °C⁻¹ to 28.37x10⁻³ Wm⁻² °C⁻¹ for Pyramid still under three modes of study. Water temperature and thermal conductivity increase with respect to time and possess almost the same trend. Performance ratio observed for pyramid solar still under three modes of study found to be in the range of 2.11 % to 7.25 %, 2.64 % to 8.66 % and 2.72 % to 11.27 % respectively. Performance ratio value is increasing steadily with respect to water temperature. It is inferred that the coupling effect of flat plate collector and shallow solar pond with the still causes the increase in temperature to the optimum value for evaporation.

Keywords: Solar Still, Temperature, Distillate Yield, Flat Plate Collector, Shallow Solar Pond

1. Introduction

Nowadays the demand for freshwater is at its peak due to the result of population explosion and rapid development in industrial sector. As a result of it, global energy demand had increased to meet the daily requirements [1, 2]. Lack of freshwater problem is solved by seawater desalination using the fossil fuels produce the dangerous polluting gases. Thus, the alternate to this environmental problem is by means of using the renewable energy [3]. More focus on renewable energy sources such as solar, geothermal, hydropower, OTEC, wind and bioenergy minimises the environmental impact of fossil fuels [4, 5]. In regions of high water contaminated areas, ground water cannot be directly used for domestic purpose due to the

* Corresponding Author

e-mail:solarselva@gmail.com

presence of heavy metals, salt, bacteria and other contaminants. Alternate solution for providing the fresh water in the exploited zone is the solar desalination. It is process of using solar thermal energy to convert the brackish water to potable one [6, 7]. Due to the simple mechanism and passive nature, solar desalination is found to be the best way of providing water with good quality for small scale domestic purpose [8]. Enormous researches had been carried out regarding the capability and analysis of desalination methods [9, 10]. Results inferred that daily around 65 million m³/day distillate yield achieved and is used for industrial and domestic needs [11]. Impact of heat and mass transfer on the water depth in the basin area of a passive solar still has been analyzed detailly [12, 13]. Results concluded that evaporative heat transfer is more predominant than convective and radiative heat transfer modes.

Efficiency, heat transfer coefficient and pumping power for flat plate solar collector along with various absorber tube for enhanced water heater under various modes had been investigated [14, 15, 16]. Results concluded that flow rate have strong effect on thermal efficiency of FPC. Role of nanofluid in enhancing the thermophysical properties had been carried out [17, 18]. It is observed that the performance of the solar collector is enhanced to higher level. Impact of flat plate collector in enhancing the distillate yield of conventional solar still had been studied along with influence of design factors and ambient conditions on efficiency [19, 20, 21]. It is inferred that the productive yield is improved around 1.3 to 2 times than that of conventional still productivity. Theoretical and experimental analysis of possible modes of heat extraction had been analysed [22-25]. Experiments concluded that SSP could provide 88 litres of hot water at a maximum temperature of 60 °C at sunset. Also, SSP can retain temperature of 47 °C till 7.00 a.m. next day which is appropriate for domestic applications. It also concludes that additional glass cover reduces both the top and total loss coefficients by 54 and 44%, respectively. Effect of shallow solar pond in enhancing the distillate yield of basin type solar still is investigated [26-28]. Results concluded that performance of modified basin still yield is comparatively higher that compared with conventional basin type still under same weather and operating conditions. Conservation of energy is used for theoretical analysis and the obtained results inferred a very good agreement with the experimental study.

The aim of this work is to study the enhanced performance of a pyramid solar still with coupled with flat plate collector (FPC) and shallow solar pond (SSP). Solar still is one of the prevalent methods used to convert saline water to potable water. FPC is coupled with solar still for instantaneous transfer of heat energy to solar still, whereas SSP is coupled to still for heat transfer at off sunshine hours. As a result of combination of two different modes of heat transfer to Pyramid solar still, its distillate yield and performance variation is observed and tabulated.

2. Construction Details

2.1 Construction of Pyramid Solar Still

Pyramid solar still of area 0.50 m x 0.50 m is designed using mild steel. Acrylic sheet 3mm thickness is used as the top cover for the still, which is placed over the grooves provided at all sides for uniform resting along with cushion supports. Bottom and sides of the basin are painted with black paint for good absorption of solar radiation and is filled with water to a height of 0.05 m. Two pipes are placed at a height of 0.06 m and 0.11 m respectively to maintain the water level inside the storage basin as 0.05 m and 0.10 m respectively. Water Collection segment is placed at the end of the still for collecting the evaporated water and it is of dimension 0.66 m x 0.038 m x 0.015 m. Outer box of the still is made up of wood of thickness 4mm with the dimension 0.70 m x 0.70 m. Sawdust and glass wool insulation are provided at bottom and side for minimizing the heat loss through it. Bushes are placed at the base of the still for uniform landing in the ground.

2.2 Construction of Flat Plate Collector

Copper sheet of 2 mm thickness of is used as absorber plate and is coated with black paint of 300 μm thickness to increase the efficiency of absorption. Total area of absorber plate is of dimension 0.82 m x 0.82 m. Eight vertical heat exchangers with distance of 0.10 m are fused together with the bottom and top tubes also to the absorber plate with perfect copper soldering act as liquid heat exchanger. Inlet is provided at the bottom of the header arrangement and outlet at top of the header arrangement. To increase the contact area of the absorber plate with copper tube, the absorber is clamped in such a way that the copper tube is completely covered by itself. The unclamped area of the absorber over the copper tube is soldered properly. This work is done in order to enhance the transferring of heat energy from absorber to the fluid passing through the tubes. Transparent glass sheet of thickness 3 mm is used as the top cover. Absorber plate along with the copper tube arrangement is properly fitted with the wooden frame made up off wood in order to prevent the bending of the absorber plate during the experimental study. Bottom surface of the wooden box is filled with glass wool about 0.10 m. A steel stand with the inclination of about 45°C is specially designed to hold the entire arrangement of the flat plate collector.

2.3 Construction of Shallow Solar Pond

General dimension of the shallow solar pond is 1 m x 1 m x 0.15 m. Pond is filled with the water to a height of 0.05 m and the surface is covered by a transparent polythene sheet. The

top of the system is covered by a glass plate with wooden frames. It is tightened using bolts provided at the surface of the wall with cushions. Cushions are used to reduce the air leakage. Bottom of the pond is insulated by using thermocole (Insulator). Its sides are covered with the help of bricks and cement mortar. Pre-calibrated thermocouples are placed at height of 0.15 m, 0.45 m and 0.60 m for measuring the temperatures at various places. The gap between insulation layer and bricks wall is filled by pieces of thermocole.

3 Thermal Performance Study

Thermal performance study of acrylic pyramid solar still is carried out from 9 a.m. to 5 p.m. for several weeks. Initially the still basin is filled with 15 litres of saline water. Thermal performance is carried out in three different modes namely

- a) Pyramid Solar Still alone
- b) Pyramid Solar Still Coupled with FPC
- c) Pyramid Solar Still Coupled with SSP

By placing pre-calibrated thermocouples at appropriate places, ambient temperature (T_{amb}), air temperature inside the still (T_a), water temperature inside the still (T_w), top acrylic cover temperature (T_c) are measured along with total solar insolation (I_s) at regular time intervals. Amount of distilled water collected for unit time per unit area is calculated using

$$M_w = \frac{Q_{ew}}{L} \quad (1)$$

Acrylic cover absorbs the incoming radiation and a small portion is reflected by it. Small portion heat is leaked through the bottom and sides of basin. Remaining portion of heat is used to raise the temperature of water, which causes evaporation. Efficiency of the still is calculated using the relation

$$\eta = \left(\frac{M L}{I_s A t} \right) \quad (2)$$



Fig (1) Pyramid Solar Still

A simple theory for the performance of flat plate collector was developed by Hottel, Woertz, Whiller and Bliss (HWB) method. The analysis assumes a steady state situation in which the liquid flows through the tubes bonded on the underside of the absorber plate. Instantaneous collector efficiency is given by,

$$\eta = \left(\frac{q_u}{A_p I_s} \right) \quad (3)$$



Fig (2) Pyramid Solar Still with Flat Plate Collector

Performance study of the pond is studied by filling the pond with 5cm thickness of water layer. Surface of the water is covered by using transparent polythene sheet and it acts as evaporation suppresser. Volume occupied by this layer is 39 liters. Hourly rise in temperature of the pond, solar radiation and ambient temperature are measured. Heat extraction is carried from pond by keeping flow rate as constant. Efficiency of SSP is defined according to HWB equation as rate of heat collection per unit SSP area (q) to the solar radiation incident on the surface of the pond. The hourly collection efficiency of a SSP is defined as

$$\eta = \left(\frac{q}{I_s} \right) \quad (4)$$



Fig (3) Pyramid Solar Still with Shallow Solar Pond

4. Heat Transfer Modes in Solar Still

Heat and mass transfer coefficients for normal range of operation of a conventional solar still is proposed by R.V. Dunkle [29]. Heat is transported inside the still by free convection of air. It releases its enthalpy upon air coming into contact with the acrylic cover. Heat transfer per unit area per unit time due to convection is,

$$Q_{cw} = 0.884 \left[(T_w - T_g) + \left(\frac{(P_w - P_g)(T_w + 273)}{268.9 \times 10^3 - P_w} \right)^{1/3} \right] (T_w - T_g) \quad (5)$$

Dunkle connects convective and evaporation heat transfer coefficients as

$$Q_{ew} = 16.273 \times 10^{-3} h_{cw} R_1 (T_w - T_g) \quad (6)$$

Using Stefan Boltzmann's constant, the Radiative heat transfer coefficient is given by,

$$Q_{rw} = \sigma \varepsilon \left[(T_w + 273)^4 - (T_g + 273)^4 \right] \quad (7)$$

Due to the small thickness of the top cover, it is assumed that the lamp of the cover is uniform. Therefore, external convection loss from top cover to the outside atmosphere is calculated using

$$Q_{ce} = h_{ca} (T_g - T_a) \quad (8)$$

here, h_{ca} is a function of wind velocity and is given by J.A. Duffie and W.A. Beckman [30].

External radiation loss from the acrylic cover to the atmosphere is given by,

$$Q_{re} = \varepsilon_g \sigma \left[(T_g + 273)^4 - (T_{sky} + 273)^4 \right] \quad (9)$$

Similarly, the external bottom loss from basin through base and sides is given by

$$Q_{be} = h_b (T_b - T_a) \quad (10)$$

Experimentally measured temperatures of evaporation and condensation surfaces are used to calculate the thermophysical properties.

$$k = 0.0244 + (0.7673 \times 10^{-4}) T_{av} \quad (11)$$

$$\mu = (1.718 \times 10^{-5}) + (4.620 \times 10^{-8}) T_{av} \quad (12)$$

$$\rho = 353.44 / (273.35 + T_{av}) \quad (13)$$

5. Result and Discussion

The performance of the Pyramid solar still is analysed and also combined with shallow solar pond and flat plate collector. Radiative heat transfer (Q_{ri}), convective heat transfer (Q_{ci}) and evaporative heat transfer (Q_{ei}) under internal heat transfer modes are predicted. Similarly, external heat transfer modes by conduction heat transfer (Q_{be}), external heat transfer through radiation from the glass cover (Q_{re}) and heat transfer from acrylic cover to atmosphere by convection (Q_{ce}) are also estimated. Instantaneous efficiency, performance ratio, saturation vapour pressure and latent heat parameters are also calculated for the Pyramid solar still, which is combined with flat plate collector and shallow solar pond. Thermophysical properties of water such as thermal conductivity, density and viscosity are also estimated for three modes of analysis. Readings are recorded for number of clear sky days and almost equal average radiation received during the three studies are considered for the analysis and reported.

Fig (4) shows the variation of temperature for water, air, inner surface of the cover, outer surface of the cover and ambient with respect to time in Pyramid solar still performance study. The maximum rise in water and air temperature inside the still is observed as 55.5 °C and 58.5 °C. Variation of ambient temperature is in the range of 32 °C to 37 °C during the study. Similarly, the variation of top cover temperature is in the range of 32 °C to 44 °C. Normally, the rise in top cover temperature affects the condensation of water vapor over the top cover.

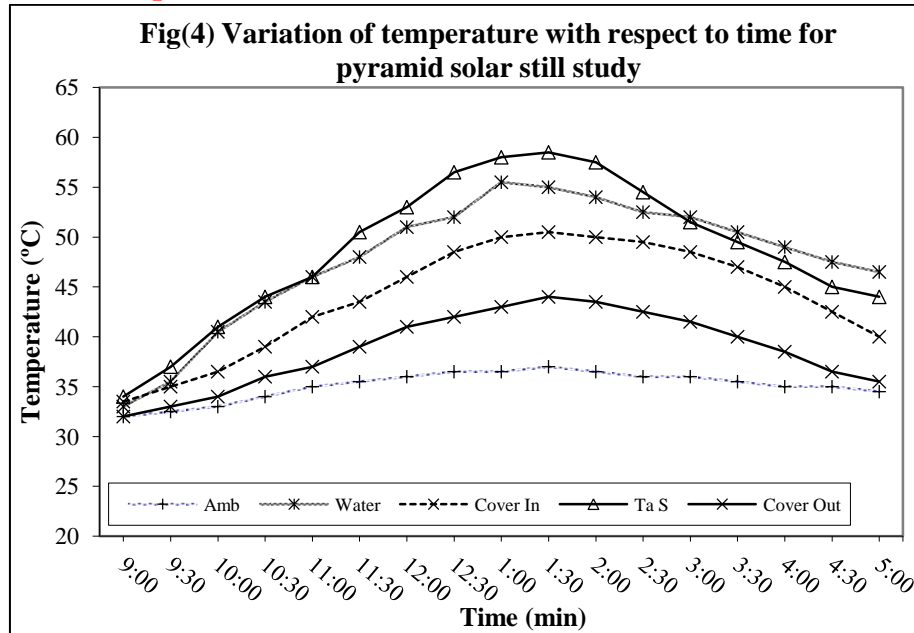


Fig (5) shows the variation of temperature for water, air, inner surface of the cover, outer surface of the cover of the still, water inlet and water outlet temperature of the flat plate collector and ambient temperature with respect to time in the pyramid solar still performance combined with flat plate collector. The water temperature of the pyramid solar still rises during the initial sunshine hours and it decreases due to decrease of radiation intensity. Maximum rise in water and air temperature is observed as 61 °C and 63 °C. Variation of ambient temperature is in the range of 33 °C to 37.5 °C during the study. Similarly, the variation of top cover temperature is in the range of 33 °C to 45.5°C. Flat plate collector inlet water temperature is in the range of 33 °C to 60.5 °C and 33.5 °C to 61 °C for outlet water temperature.

Due to the thermosyphon effect, heat energy is transferred from the flat plate collector to the pyramid solar still. This process is confirmed by analyzing the temperature of the inlet, outlet and water temperature of the still. Therefore, water temperature of the still increases simultaneously along with the inlet and outlet water temperature of the still with respect to time and maintains inlet and outlet temperature almost a nearer value during 12.30 a.m. to 3.30 p.m. Collection rate is more only during 3.00 p.m. to 5.00 p.m. due to thermosyphon effect. Finally, the yield reduces in the evening due to the decrease of water temperature and evaporation rate. At off sunshine hours, water circulation to and from the flat plate collector is closed by using separate valves.

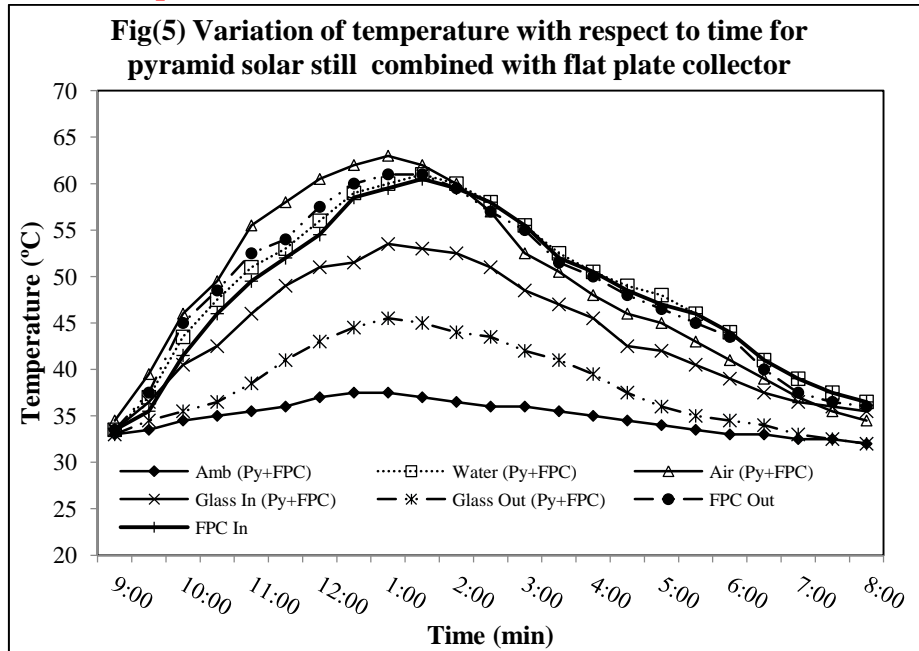


Fig (6) shows the variation of temperature for water, air, inner surface of the cover, outer surface of the cover of Pyramid solar still, water temperature of pond, water inlet and water outlet temperature of the shallow solar pond and ambient temperature with respect to time in Pyramid solar still performance combined with shallow solar pond. Variation of ambient and top cover temperature is in the range of 32 °C to 37 °C and 33 °C to 45°C. Maximum rise in water and air temperature of solar still is observed as 58.5 °C and 62 °C. Inlet and outlet water temperature of the shallow solar pond is in the range of 33 °C to 58.5 °C and 34 °C to 58.5 °C. Similarly, the maximum air and water temperature inside shallow solar pond is about 70 °C and 70.5 °C. Water temperature inside the still is maintained even at off sunshine hours due to due to the circulation of water through the shallow solar pond. As a result, distillate yield obtained from the still is not slowed even at off sunshine hours. The yield rate difference is more for the regular intervals measured between 2.00 p.m. and 5.00 p.m. and finally the yield starts to reduce after 11.00 p.m. due to the decrease of water temperature and evaporation rate.

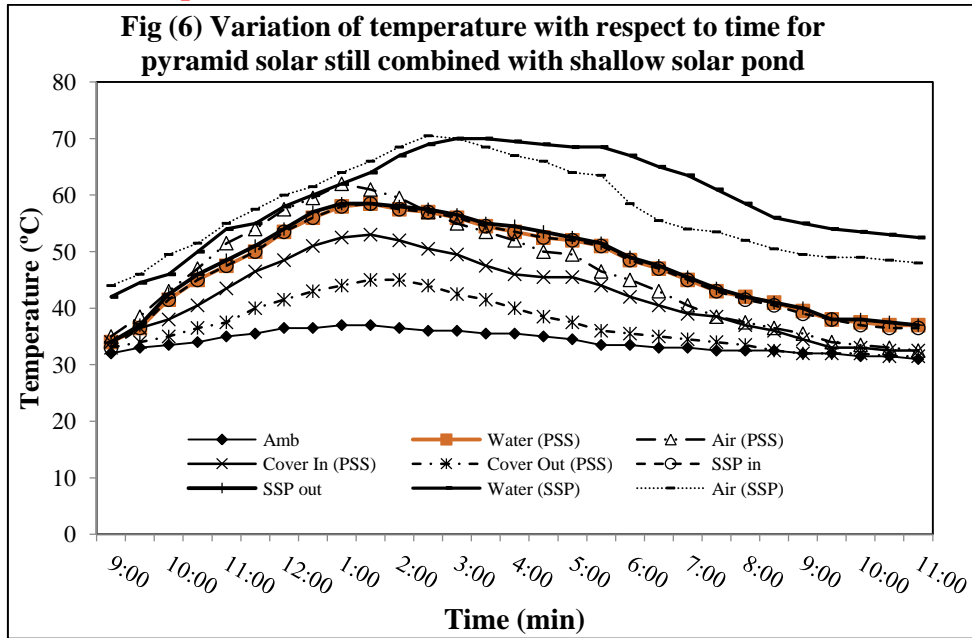
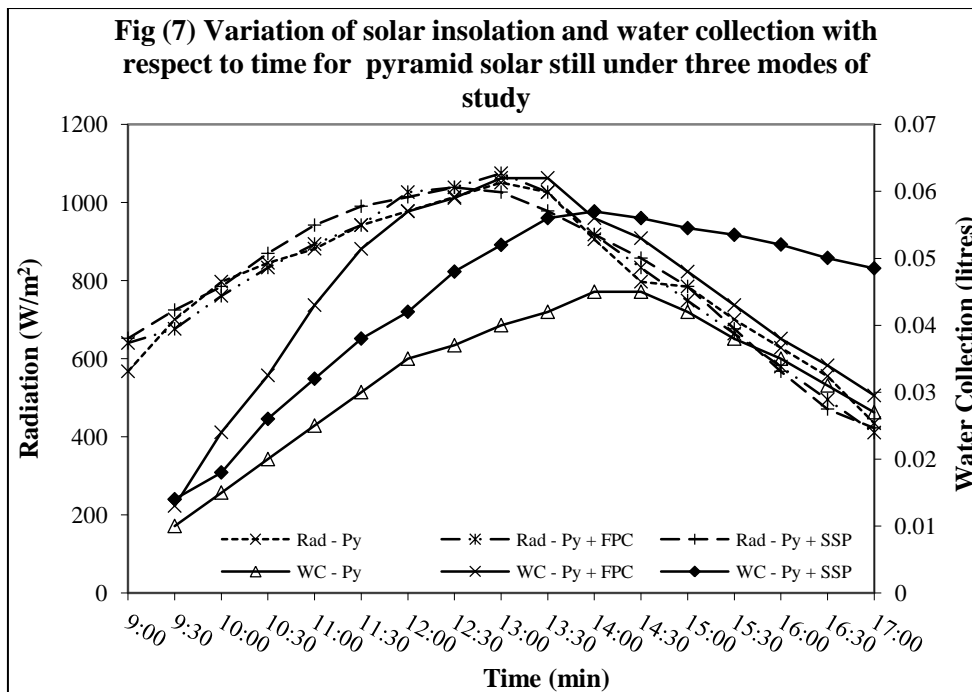


Fig (7) shows the variation of solar radiation and water collection with respect to time for the pyramid solar still under three modes of study. Radiation increases linearly with time and reaches the maximum value from 12 p.m. to 2 p.m. and then decreases.



Radiation received during this study is in the range of 96.62 W/m² to 1050.69 W/m², 96.62 W/m² to 1074.85 W/m² and 96.62 W/m² to 1038.62 W/m² for pyramid still performance study under three modes of study with average radiation of 766.88 W/m² during the study. Variation of distilled water collection observed is in the range of 0.01 kg to 0.045 kg, 0.013 kg to 0.062 kg and 0.014 kg to 0.057 kg for the Pyramid still performance study under three modes of study. Water collection is increased linearly during the initial hours even though the

instantaneous yield rate at regular intervals is less because the initial radiation is completely utilized for the warm up temperature than the distillate yield. Due to instantaneous heat transfer from FPC, enhanced distillate output is observed during sunshine hours. Due to continuous heat gain from the shallow solar pond, water collection is maintained even at off shine hours due to the coupling effect.

Fig (8) shows the variation of instantaneous efficiency and performance ratio with respect to time for performance study of pyramid solar still under three modes of study. Instantaneous efficiency observed during the study is in the range of 7.52% to 30.73%, 2.41% to 9.01% and 2.42% to 11.28% for the pyramid still performance study alone, combine with FPC and combined with SSP. Efficiency of the combined performance is found to be less because the total area of the combined system is larger than the still area. Even though the instantaneous efficiency in this mode is reduced than the pyramid solar still, the distillate water collection rate is increased. Performance ratio observed for pyramid solar still under three modes of study found to be in the range of 2.11 % to 7.25 %, 2.64 % to 8.66 % and 2.72 % to 11.27 % respectively. Performance ratio value is increasing steadily with respect to water temperature. It is inferred that the coupling effect of flat plate collector and shallow solar pond with the still causes the increase in temperature to the optimum value for evaporation.

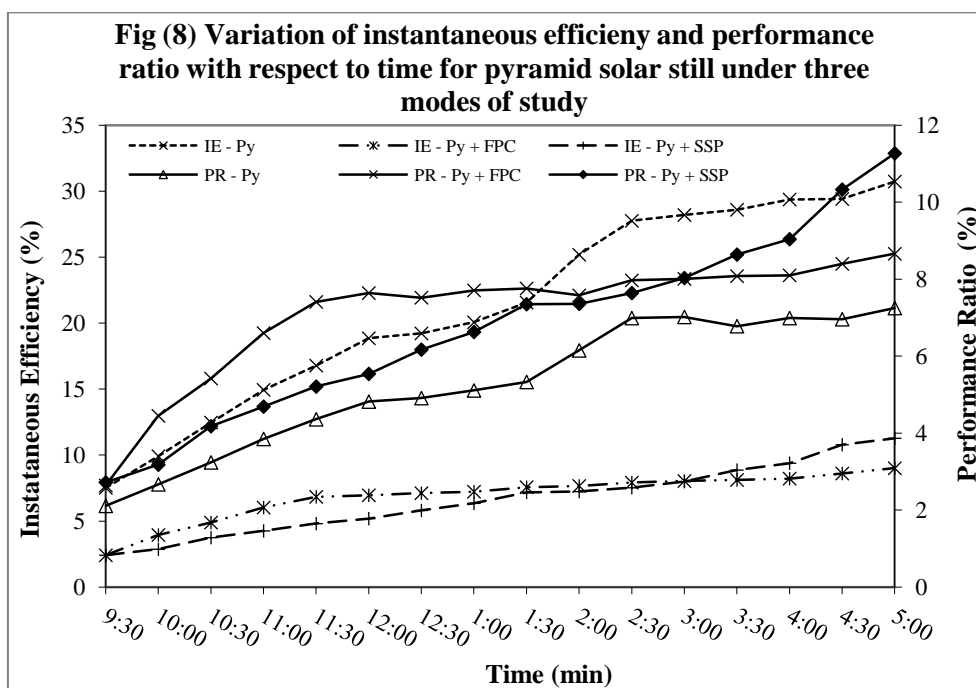


Fig (9) shows the variation of water temperature and thermal conductivity with respect to time. Water temperature rises with respect to incident radiation and is found to be in the range of 55.5 °C, 61 °C and 58.5 °C for all the three modes of study. Instantaneous increase in water temperature is observed in case of still with FPC due to the coupling effect. Whereas in case of

still coupled with SSP, water temperature is maintained even at off sunshine hours due to thermosyphon effect. Thermal conductivity of water is analyzed and it is observed in the range of $26.89 \times 10^{-3} \text{ Wm}^{-2} \text{ }^\circ\text{C}^{-1}$ to $28.19 \times 10^{-3} \text{ Wm}^{-2} \text{ }^\circ\text{C}^{-1}$, $26.95 \times 10^{-3} \text{ Wm}^{-2} \text{ }^\circ\text{C}^{-1}$ to $28.46 \times 10^{-3} \text{ Wm}^{-2} \text{ }^\circ\text{C}^{-1}$ and $26.97 \times 10^{-3} \text{ Wm}^{-2} \text{ }^\circ\text{C}^{-1}$ to $28.37 \times 10^{-3} \text{ Wm}^{-2} \text{ }^\circ\text{C}^{-1}$ for pyramid still under three modes of study. Water temperature and thermal conductivity increase with respect to time and possess almost the same trend. It is inferred that the density of water increases with respect to increase in water temperature and it starts to decrease as water temperature decreases.

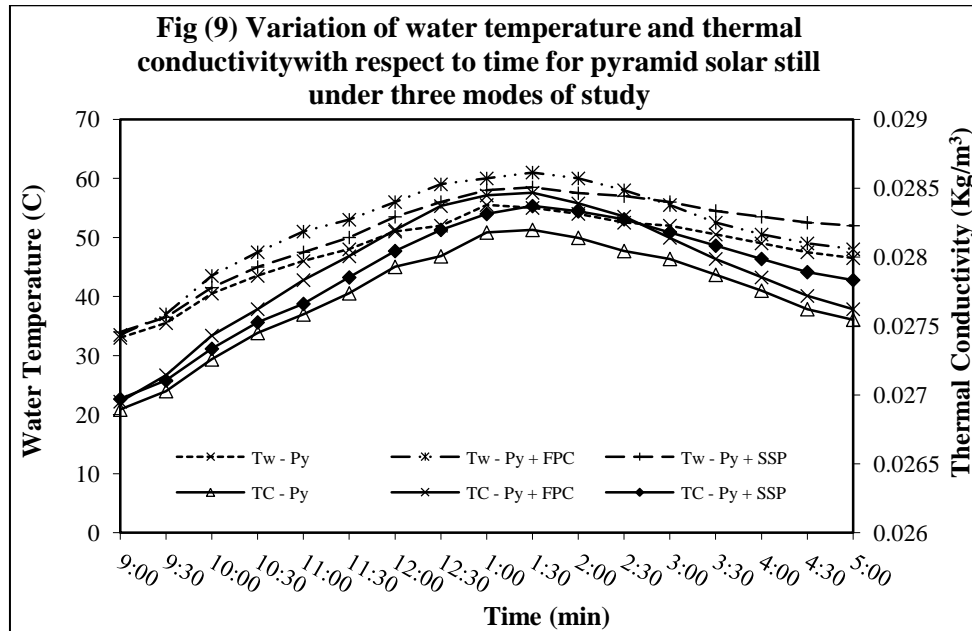
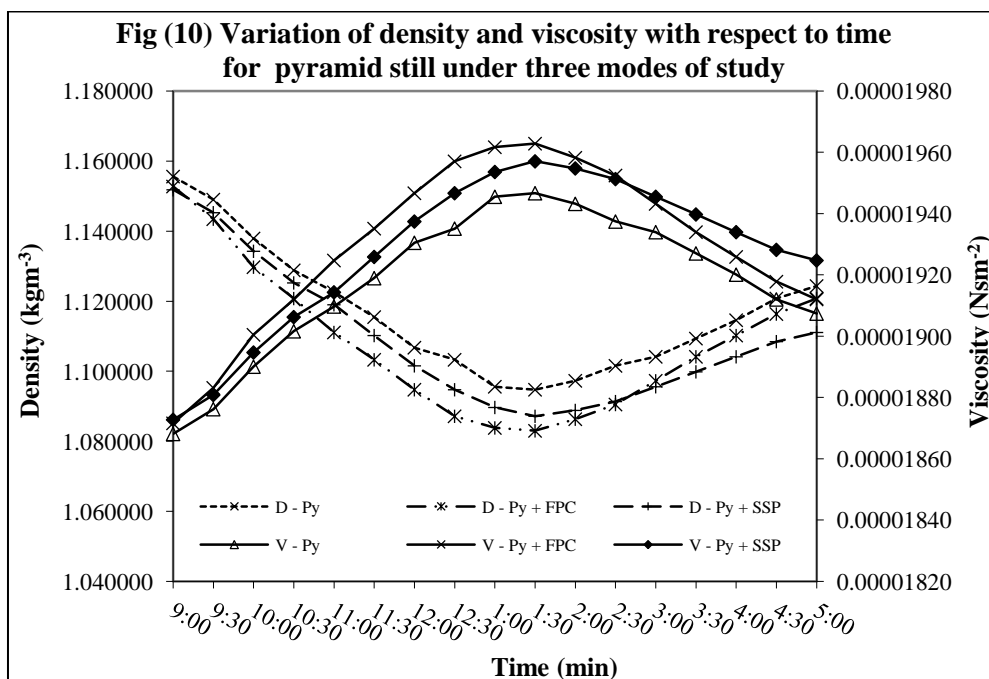
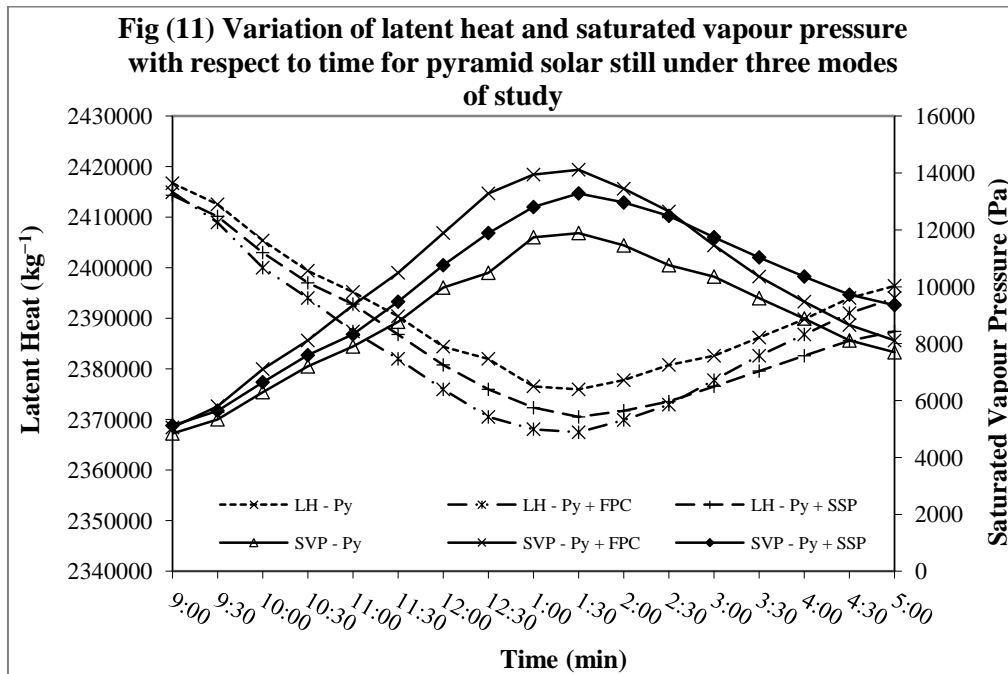


Fig (10) shows the variation of dynamic viscosity and density of water with respect to time. The dynamic viscosity of water is predicted in the range of $18.68 \times 10^{-6} \text{ Nsm}^{-2}$ to $19.47 \times 10^{-6} \text{ Nsm}^{-2}$, $18.72 \times 10^{-6} \text{ Nsm}^{-2}$ to $19.63 \times 10^{-6} \text{ Nsm}^{-2}$ and $18.73 \times 10^{-6} \text{ Nsm}^{-2}$ to $19.57 \times 10^{-6} \text{ Nsm}^{-2}$ for



pyramid still under three modes of study. Density of water is predicted for still under three modes of study and it is observed as $11.55 \times 10^{-1} \text{ kgm}^{-3}$ to $10.94 \times 10^{-1} \text{ kgm}^{-3}$, $11.52 \times 10^{-1} \text{ kgm}^{-3}$ to $10.83 \times 10^{-1} \text{ kgm}^{-3}$ and $11.51 \times 10^{-1} \text{ kgm}^{-3}$ to $10.87 \times 10^{-1} \text{ kgm}^{-3}$. It concludes that the density decreases with respect to increase in viscosity and it starts to increase with the decrease in viscosity.

Fig (11) shows the variation of saturation vapour pressure and latent heat inside the Pyramid still for three modes of studies. Saturation vapour pressure reaches maximum value when water collection is more and tends to decrease when water collection decreases.



Saturation vapour pressure is predicted in the range of 4842.65 Pa to 11889.52 Pa, 5050.66 Pa to 14114.04 Pa and 5121.7 pa to 13281.98 Pa for pyramid solar still under three modes of study. Difference in saturated vapour pressure is very less at higher temperature compared to the warm up period. Latent heat value is found to increase when the saturation vapour pressure starts to decrease. It concludes that the latent heat is decreased at higher order of temperature. Latent heat value observed is in the range of 2416722.46 to 2375960.52 kg⁻¹, 2414936.96 to 2367475.98 kg⁻¹ and 2414341.57 to 2370510.43 kg⁻¹ for pyramid solar still under three modes of study. Latent heat is fully utilized for boosting the condensation commencing at lower temperature from 9.00 a.m. to 1.30 p.m. Thus, the effect of latent heat is not completely utilized for condensation at higher temperatures.

In the solar still, the evaporative heat transfer coefficient (Q_{ei}) is the major heat loss and is greater than the other two modes together. It is observed that the radiative heat transfer coefficient (Q_{ri}) and convective heat transfer coefficient (Q_{ci}) do not vary much in comparison to

evaporative heat transfer coefficient (Q_{ei}). This indicates the strong dependence of evaporative heat transfer coefficient (Q_{ei}) on the operating water temperature (T_w).

Table: 1: Heat Transfer Values:

	Q_{ci} (W/m ²)	Q_{ri} (W/m ²)	Q_{ei} (W/m ²)	Q_{ce} (W/m ²)	Q_{re} (W/m ²)	Q_{be} (W/m ²)
Pyramid Solar Still	14.28	47.97	114.46	32.13	77.84	4.35
Pyramid Solar Still combined with Flat Plate Collector	17.57	57.07	156.15	38.71	84.08	5.32
Pyramid Solar Still combined with Shallow Solar Pond	19.06	60.22	160.86	33.66	79.22	5.98

Table: 2: Thermophysical Properties:

	Thermal Conductivity (Wm ⁻² °C ⁻¹)	Dynamic Viscosity (Nsm ⁻²)	Density (kgm ⁻³)
Pyramid Solar Still	26.89x10 ⁻³ to 28.19x10 ⁻³	18.68x10 ⁻⁶ to 19.47 x10 ⁻⁶	11.55x10 ⁻¹ to 10.94x10 ⁻¹
Pyramid Solar Still combined with Flat Plate Collector	26.95x10 ⁻³ to 28.46x10 ⁻³	18.72x10 ⁻⁶ to 19.63x10 ⁻⁶	11.52x10 ⁻¹ to 10.83x10 ⁻¹
Pyramid Solar Still combined with Shallow Solar Pond	26.97x10 ⁻³ to 28.37x10 ⁻³	18.73x10 ⁻⁶ to 19.57x10 ⁻⁶	11.51x10 ⁻¹ to 10.87x10 ⁻¹

Conclusion:

The performance of the Pyramid solar still combined with flat plate collector and shallow solar pond is studied. The effect of water temperature in the still causes the increase in distillate yield. The combined performance results confirmed that even smaller surface area of the top cover in the still can also produce more distillate yield. Saturation vapour pressure and latent heat also plays a major role in production of distillate yield. Overall distillate yield and performance of Pyramid solar still coupled with FPC and SSP is found to be more than that of single slope solar still coupled with FPC and SSP.

Reference:

[1] Y. Tripanagnostopoulos, T.H. Nousia, M. Souliotis, and P. Yianoulis, "Hybrid Photovoltaic/Thermal Solar Systems", Solar Energy, vol. 72, issue. 3, pp. 217-234, 2002.
 [2] Y. Zhang, M.S. Yang, K. Enever and M. Ramezani-pour, "Application of Solar Energy in Water Treatment Processes: A Review", Desalination, vol. 428. 116-145, 2018.

- [3] A. Subramani, M. Badruzzaman, J. Oppenheimer and J.G. Jacangelo, J.G., “Energy Minimization Strategies and Renewable Energy Utilization for Desalination: A Review”, *Water Research*, vol. 45, pp. 1907-1920, 2011.
- [4] Zhao, Zhen-Yu, Chen and Yu-Long, “Critical Factors Affecting the Development of Renewable Energy Power Generation: Evidence from China”, *Journal of Cleaner Production*, vol. 184, pp. 466-480, 2018.
- [5] Milano, Jassinnee, Ong, Hwai Chyuan, Masjuki, H.H., Chong, W.T., Lam, Man Kee, Loh, Ping Kwan, Vellayan and Viknes, “Microalgae Biofuels as an Alternative to Fossil Fuel for Power Generation”, *Renewable Sustainable Energy Reviews*, vol. 58, pp.180-197, 2016.
- [6] A. Pugsley, A.Z. Jayanta, D. Mondol and M. Smyth, “Global Applicability of Solar Desalination”, *Renewable Energy*, vol. 88, pp. 200-219, 2016.
- [7] V.G. Gude, N. Nirmalakhandan and S. Deng, “Renewable and Sustainable Approaches for Desalination. *Renewable and Sustainable Energy Reviews*, vol.14, issue. 9, pp. 2641-2654, 2010
- [8] B. Boucekima, ‘A Solar Desalination Plant for Domestic Water Needs in Arid Areas of South Algeria’, *Desalination*, vol. 153, pp. 65-69, 2003.
- [9] G.N. Tiwari and L. Sahota, “Advanced Solar Distillation Systems”, Springer Singapore; 2017.
- [10] E. Delyannis, “Historic Background of Desalination and Renewable Energies”, *Solar Energy*, vol. 75, issue. 5, pp. 357-366, 2003.
- [11] A. R. Hoffman, “Water Security: A Growing Crisis and the Link to Energy”, *AIP Conf. Proc.* vol.1044, issue. 1, pp. 55-63, 2008.
- [12] A.K. Tiwari and G.N. Tiwari, “Thermal Modelling Based on Solar Fractions and Experimental Study of the Annual and Seasonal Performance of a Single Slope Passive Solar Still: The Effect of Water Depths”, *Desalination*, vol. 207, pp. 184-204, 2007.
- [13] B. Selva Kumar, Sanjay Kumar and R. Jayaprakash, “Performance Analysis of a “V” Type Solar Still Using a Charcoal Absorber and a Boosting Mirror”, *Desalination*, vol. 229, pp. 217-230, 2008
- [14] K. Balaji, S. Iniyani and V. Muthusamyswami, “Experimental Investigation on Heat Transfer and Pumping Power of Forced Circulation Flat Plate Solar Collector using Heat Transfer Enhancer in Absorber Tube”, *Applied Thermal Engineering*, vol. 1125, pp. 237-247, 2017.
- [15] Q. Yu, M. Hu, J. Li, Y. Wang and G. Pei, “Development Of A 2D Temperature-Irradiance Coupling Model For Performance Characterizations Of The Flat-Plate Photovoltaic/Thermal (PV/T) Collector”, *Renewable Energy*, vol. 153, pp. 404-419, 2020.
- [16] Kheira Tabet Aoul, Ahmed Hassan, Ali Hasan Shah and Hassan Riaz, “Energy Performance Comparison of Concentrated Photovoltaic – Phase Change Material Thermal (CPV-PCM/T) System with Flat Plate Collector (FPC)”, *Solar Energy*, vol. 176, pp. 453-464, 2018.
- [17] Pankaj Raj and Sudhakar Subudhi, “A Review of Studies Using Nanofluids in Flat-Plate and Direct Absorption Solar Collectors”, *Renewable and Sustainable Energy Reviews*, vol. 84, pp. 54-74, 2018.
- [18] E. B. Elcioglu, A. M. Genc, Z. H. Karadeniz, M. A. Ezan and A. Turgut, “Nanofluid Figure-of-Merits to Assess Thermal Efficiency of a Flat Plate Solar Collector”, *Energy Conversion and Management*, vol. 20415, article 112292, 2020
- [19] Jamel Madiouli, Ashraf Lashin, Ihab Shigidi, Irfan Anjum Badruddin and Amir Kessentini, “Experimental Study and Evaluation of Single Slope Solar Still Combined with Flat Plate Collector, Parabolic Trough and Packed Bed”, *Solar Energy*, vol. 19615, pp. 358-366, 2020
- [20] Raja Sekhar Dondapati, Rahul Agarwal, Vishnu Saini, Gaurav Vyas and Jitendra Thakur, “Effect of Glazing Materials on the Performance of Solar Flat Plate Collectors for Water Heating Applications”, *Materials Today: Proceedings*, vol. 5, issue 14, pp. 27680-27689, 2018
- [21] Mousa Abu-Arabi, Mohammad Al-harashseh, Maysam Ahmad and Hasan Mousa, “Theoretical Modeling of a Glass-Cooled Solar Still Incorporating PCM and Coupled to Flat Plate Solar Collector”, *Journal of Energy Storage*, vol. 29, article 101372, 2020
- [22] S. Aboul-Enein, A. A. El-Sebaili, M. R. I. Ramadan and A. M. Khallaf, “Parametric Study of a Shallow Solar-Pond Under the Batch Mode of Heat Extraction”, *Applied Energy*, vol. 78, Issue 2, pp. 159-177, 2004.
- [23] A. A. El-Sebaili, S. Aboul-Enein, M. R. I. Ramadan and A. M. Khallaf, “Thermal Performance Of Shallow Solar Pond Under Open Cycle Continuous Flow Heating Mode for Heat Extraction”, *Energy Conversion and Management*, vol. 47, Issues 7–8, pp. 1014-1031, 2006.

- [24] M. R. I Ramadan, A. A El-Sebaei, S Aboul-Enein and A. M Khallaf, "Experimental Testing of a Shallow Solar Pond with Continuous Heat Extraction", *Energy and Buildings*, vol. 36, Issue 9, pp. 955-964, 2004.
- [25] Sunirmit Verma and Ranjan Das, "Effect of Ground Heat Extraction on Stability and Thermal Performance of Solar Ponds Considering Imperfect Heat Transfer", *Solar Energy*, vol. 1981, pp. 596-604, 2020.
- [26] M. Appadurai and V. Velmurugan, "Performance Analysis of Fin Type Solar Still Integrated with Fin Type Mini Solar Pond", *Sustainable Energy Technologies and Assessments*, vol. 9, pp. 30-36, 2015.
- [27] G. S. Dhindsa, and M. K. Mittal, "Experimental Study of Basin Type Vertical Multiple Effect Diffusion Solar Still Integrated with Mini Solar Pond to Generate Nocturnal Distillate", *Energy Conversion and Management*, vol. 1651, pp. 669-680, 2018.
- [28] V. Velmurugan and K. Srithar, "Solar Stills Integrated with a Mini Solar Pond - Analytical Simulation and Experimental Validation", *Desalination*, vol. 216, Issues 1–35, pp. 232-241, 2007,
- [29] R.V. Dunkle, "Solar water distillation: roof type still and a multiple effect diffusion still, *International Development in Heat Transfer*", A.S.M.E., Proc. International Heat Transfer, Part V, University of Colorado, pp. 895, 1961.
- [30] J.A. Duffie and W.A. Beckman, "Solar energy thermal process", John Wiley and Sons, New York, U.S.A, 1974.